Cent. Eur. J. Geosci. • 2(3) • 2010 • 321-328
DOI: 10.2478/v10085-010-0021-8

VERSITA

Central European Journal of **Geosciences**

# Note on the evolution of a Miocene composite volcano in an extensional setting, Zărand Basin (Apuseni Mts., Romania)

**Communication**

Ioan Seghedi[1]*, Alexandru Szakács[12], Emilian Roşu[3], Zoltán Pécskay[4], Katalin Gméling[5]

*1 Institute of Geodynamics, Romanian Academy 19-21, Jean-Luis Calderon str., RO-020032 Bucharest, Romania*

*2 Sapienţia University, Dept. of Environmental Sciences, Matei Corvin str., 4, RO-400112 Cluj-Napoca, Romania*

*3 Geological Institute of Romania, 1, Caransebeş str., RO-78344 Bucharest, 32, Romania*

*4 Institute of Nuclear Research of the Hungarian Academy of Sciences, P.O. Box 51, Bem ter 18/c, H-4001 Debrecen, Hungary*

*5 Institute of Isotopes, Hungarian Academy of Sciences, 29-33, Konkoly Thege-M. str., H-1121 Budapest, Hungary*

**Received 30 April 2010; accepted 17 June 2010**

**Abstract:** Bontău is a major eroded composite volcano filling the Miocene Zărand extensional basin, near the junction between the Codru-Moma and Highiş-Drocea Mountains, at the tectonic boundary between the South and North Apuseni Mountains. It is a quasi-symmetric structure (16-18 km in diameter) centered on an eroded vent area (9×4 km), buttressed to the south against Mesozoic ophiolites and sedimentary deposits of the South Apuseni Mountains. The volcano was built up in two sub-aerial phases (14-12.5 Ma and 11-10 Ma) from successive eruptions of andesite lava and pyroclastic rocks with a time-increasing volatile budget. The initial phase was dominated by emplacement of pyroxene andesite and resulted in scattered individual volcanic lava domes associated marginally with lava flows and/or pyroclastic block-and-ash flows. The second phase is characterized by amphibole-pyroxene andesite as a succession of pyroclastic eruptions (varying from strombolian to subplinian type) and extrusion of volcanic domes that resulted in the formation of a central vent area. Numerous debris flow deposits accumulated at the periphery of primary pyroclastic deposits. Several intrusive andesitic-dioritic bodies and associated hydrothermal and mineralization processes are known in the volcano vent complex area. Distal epiclastic deposits initially as gravity mass flows and then as alluvial volcaniclastic and terrestrial detritic and coal filled the basin around the volcano in its western and eastern part.

Chemical analyses show that lavas are calc-alkaline andesites with $SiO_2$ ranging from 56–61%. The petrographical differences between the two stages are an increase in amphibole content at the expense of two pyroxenes (augite and hypersthene) in the second stage of eruption; CaO and MgO contents decrease with increasing $SiO_2$. In spite of a ~4 Ma evolution, the compositions of calc-alkaline lavas suggest similar fractionation processes. The extensional setting favored two pulses of short-lived magma chamber processes.

**Keywords:** composite volcano • Apuseni Mountains • andesite • extensional setting



*E-mail: seghedi@geodin.ro

# 1. Introduction

In the Apuseni Mountains, Neogene magmatism produced four NW-SE volcano-intrusive areas [1], between 14.7 to 7.4 Ma and ended with a brief small-volume eruption at ~1.6 Ma (Uroi) [1–3]. The studied volcano is situated at the junction between the Codru-Moma and Highiş-Drocea Mts., at the tectonic boundary between the South and North Apuseni tectonic units (see inset Figure 1) [4–6]. An extensional regime in the Apuseni area during Middle Miocene time [4, 7, 8] was responsible for magma generation due to decompression melting of upper lithosphere/lower crust during eastward translation and clockwise rotation of the Intra-Carpathian blocks [1, 9–11]. This was probably coupled to asthenosphere upwelling and a higher thermal regime favoring partial melting and mixing processes [1, 11]. The largest continuous volcanic area is ca. 100 km across and developed mainly in the Zărand depression, a continuation of the Békés Basin to the west in Hungary [8, 12] (Figure 1). Although there are numerous geological studies concerning this basin [13, 14] which evolved during Miocene times, only few authors considered the volcanological aspects. Previous studies were focused on the petrography and geochemistry [15, 16]. Based on borehole data, [17, 18] the intrusive rocks and associated hydrothermal alteration and mineralization processes that occur in the central part of the volcanic structure (vent-complex) were discussed, naming it a caldera (i.e. Talagiu caldera) without referring to any clear evidence of volcanic collapse origin.

This note focused on the first volcanological interpretations of the largest composite volcano that fills the Zărand basin between Codru-Moma Mts. to the north and Highiş-Drocea Mts. to the south (Figure 1). We named this composite volcano "Bontău volcano" after its highest peak (~824 m). In support of our volcanological observations, we present seven new K-Ar age determinations, petrography and major element geochemistry of the constituent volcanic rocks.

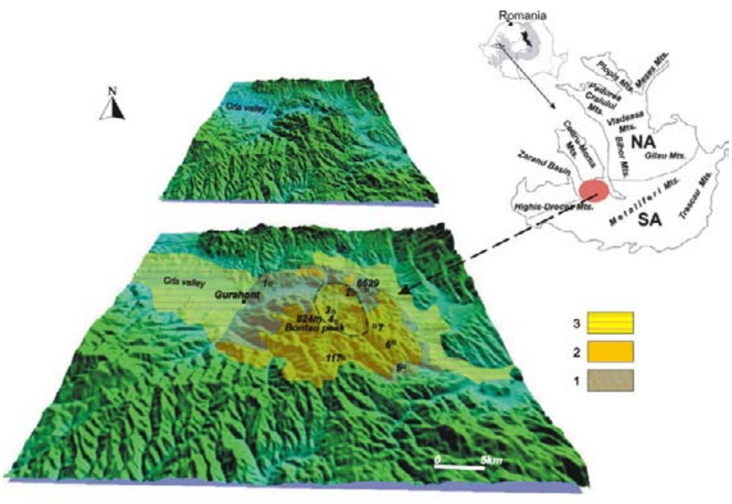


**Figure 1.** 3D image of the Bontău volcano and the surrounding areas, with a simplified geology of the volcano and K/Ar sample-points, named in Table 1 as current numbers for the new data and with original sample numbers for previously published data; Legend: 1. First phase represented by volcanic deposits dominated by pyroxene andesites- proximal and medial facies; 2. Second phase with amphibole-pyroxene andesites- proximal and medial facies; 3. Ring-plane association with distal epiclastic deposits associated with terrestrial fluvial deposits developed in the Zărand Basin in its eastern and western parts. The inset shows the position of the volcano in the Zărand Basin between the two main tectonic units of the Apuseni Mts: North Apuseni (NA) and South Apuseni (SA).

# 2. Volcanological features

In this study we recorded geological profiles on outcrops along the main radial valleys cutting the volcano. We estimated a fairly good preservation of cone morphology that represented its proximal and medial facies (Figure 1). The volcano was built up in two phases showing different

**Figure 2.** A. Quarry in a pyroxene andesite lava dome, showing a succession of lava flow sequences - western part of the volcano; B. Pyroxene andesites-bearing pyroclastic block-and-ash-flow deposit, showing various size angular clasts (compact to slightly porous) in a monolithic matrix of the same composition - north-eastern part of the volcano; C. Monolithic pyroxene andesite autoclastic breccia with various size angular clast, poor in a lapilli-size matrix of the same composition - south-eastern part of the volcano; D. Marginal fragmentation of a pyroxene andesite lava flow with the appearance of vesiculated and oxidized clinker - north-eastern part of the volcano; E. Sequences in stratified debris flows deposits, of dm to m size, dominated by pyroxene andesite clasts - south-eastern slope of the volcano; F. 2 m thick-bedded matrix-supported lapilli tuff rich in cm-dm size pumice and rare scoria clasts of amphibole-pyroxene andesites, typical for pyroclastic flow deposits - south-eastern slope of the volcano; G. Cm-dm size juvenile pumice (brighter) and scorias (darker) clasts embedded in an ash-matrix characterizing a pyroclastic flow deposit - south-western part of the volcano; H. Debris flow deposits (channeling features clearly visible) represented by massive or reversely graded muddy matrix-supported sandstones and conglomerates - south-eastern slope of the volcano.

volcanological features.

The first phase was a succession of pyroxene andesite eruptions that formed scattered individual volcanic lava domes (Figure 2A) marginally associated with lava flows, autoclastic and pyroclastic breccia (Figure 2B) and secondary deposits. Several lava flows presented marginal fragmentation with the appearance of vesiculated and oxidized clinker (Figure 2D) that sometimes passed into monolithic autoclastic breccia (Figure 2C) or debris-flow deposits of the same composition (Figure 2E). It is difficult at this stage to determine the distribution of their eruptive centers; however, they seem to be spread out in a larger area covered by the products of the later central volcano. Flank lavas issued from the main central vent area are morphologically suggested by an elliptic depression (4×9 km large).

The second phase was dominated by pyroclastic deposits and associated secondary epiclastic deposits, mainly as debris flows, with amphibole-pyroxene andesite as the main lithology. Since the volcano is much more eroded in its northern part, where it has been cut by the main Criş valley which crosses the Zărand Basin from E to W, the second phase deposits are less well exposed. A summary of the main volcaniclastic facies of this phase is given in Table 1. All the pyroclastic flow deposits have a mixture of light-colored pumice and dark-colored scoria as juvenile components.

The volcano shows a conical shape and a concave-upward

**Table 1.** Summary of the main volcaniclastic facies of the second phase volcano evolution.

| Code | Brief description | Occurrence | Interpretation |
|---|---|---|---|
| A | Thick-bedded massive lapilli tuff; 2-5 m thick (Figure 2F), matrix supported; poorly sorted ash-matrix; cm-dm size amphibole-pyroxene juvenile andesite pumice and scoria (with variable dominance) (Figure 2G), sometimes normally graded; rare cm-sized pyroxene andesite lithic clast; tabular bed geometry; | Medial facies or base of the slope | Pyroclastic flow deposits (pumice/scoria-and-ash flow); Sedimentation from pyroclastic plumes (subplinan to strombolian tephra jets) and currents |
| B | Stratified tuffs; cm to dm thick beds; well sorted; mantle bedding | Ubiquitous; Proximal to medial facies | Deposition of fallout ash |
| C | Monolithic, massive, matrix supported breccia or lapilli tuffs with cm - dm size, angular, compact or slightly porous juvenile amphibole pyroxene andesite clasts | Proximal to medial facies | Pyroclastic block and ash flows; products of dome collapse |
| D | Massive or reversely graded muddy sandstones, conglomerates, rarely breccias (Figure 2H); irregular bed geometry with frequent channeling and scour surfaces; dominated by amphibole pyroxene andesites | Medial to distal facies | Debris flow generated by reworking of loose cone deposits (autoclastic breccias, pyroclastic flow deposits or block-and-ash-flow deposits) |
| E | Thin and cross-bedded sandstone; alternating coarse and fine layers with discontinuous lapilli trains; various cm sized sub-rounded clasts enclosed; low angle discordances; poorly to moderately sorted; commonly graded low angle cross lamination in lenses or pockets; well to moderately sorted (Figures 3A, B) | Medial to distal facies | Diluted debris-flow and fluvial deposits generated by traction and suspension from poorly consolidated pyroclastic flow or fall deposits reworked between eruption events |

profile typical for composite volcanoes worldwide [20] being buttressed to the south against Late Jurassic to Late Cretaceous ophiolites and sedimentary deposits of the South Apuseni tectonic unit. The volcanic cone has been affected by long-term degradation, mostly via fluvial erosion (Figure 1). The vent area has also been deeply eroded and enlarged, and probably this was the only reason it was considered as a "caldera" resulting from collapse [16]. The central vent area displays a larger central intrusion (diorite-microdiorite) associated with pervasive hydrothermal alteration and gold, base metals and copper mineralization and neck and dyke intrusions of amphibole-pyroxene andesites [17, 18]; yet the relationships between the large and small intrusions are not known; it is assumed that small intrusions are younger [18]. The basal diameter of the volcano is 16-18 km and the suggested volume is $\sim$250 km$^3$. The ring-plain apron developed in the western and the eastern parts of the volcano is represented by distal epiclastic deposits associated with terrigeneous fluvial sediments and coal, filling the central part of the Zărand Basin [13, 21] (Figure 1). These distal deposits have not yet been studied and correlated with medial and proximal facies deposits.

## 3. Lifetime of the Bontău volcano

Seven new (see their locations in Figure 1) and two previously published [2] radiometric (K/Ar) age determinations (Table 2) provide a time-span framework for volcanic activity between 13.8-10 Ma $\pm$0.33-0.45. Two samples were collected on the south-eastern slope of the volcano and another two from its central vent-complex. Analytical methods are given in the Appendix. The first phase, represented mainly by the pyroxene andesite dome and breccia, apparently occurred in a longer time interval, between 13.8-12.0 Ma (Figure 4). The available radiometric ages suggest a gap in activity. A second phase of volcanic eruptions occurred between 11 and 10 Ma $\pm$0.33-0.45. These data should be considered as preliminary and further geochronological investigations are needed.

## 4. Petrography and geochemistry

The lava flows and domes are massive and strongly porphyritic. Phenocrysts form 30-50% of the rock volume. Groundmass textures vary from vitrophyric in quenched lavas to fine intergranular (sometimes vesiculated) to larger intergranular in slowly cooled lavas and intrusive facies. Plagioclase is the most common phenocryst phase and makes up to 60-70% by volume of most rocks (Figure 3C). It has variable An contents (30-70% in microprobe analysis). Sieve texture and complex zoning are common. Clinopyroxene (augite) and orthopyroxene (hypersthene) are also common mafic mineral phases (Figures 3C, D), sometimes appearing as glomerophyric inclusions associated with plagioclase and opaque minerals. Rims of augite

**Table 2.** K/Ar data on Neogene volcanic rocks of the Bontău volcano, Zărand Basin, Apuseni Mts., Romania.

| No. Crt. | No. of K/Ar | No. of sample | Rock type | Dated fraction | K (%) | $^{40}Ar_{rad}$ (ccSTP/g) | $^{40}Ar_{rad}$ (%) | K/Ar age (Ma) and error | Location |
|---|---|---|---|---|---|---|---|---|---|
| 1 | 7732 | M10 | Apx | whole rock | 0.714 | 3.2706*10-7 | 43.7 | 11.74±0.45 | Gura văii valley |
| 2 | 7733 | M11 | Apx am | whole rock | 1.043 | 4.3318*10-7 | 49.1 | 10.65±0.39 | Aciuţa quarry |
| 3 | 7709 | M12 | Aampx | whole rock | 0.782 | 3.2674*10-7 | 58.9 | 10.71±0.36 | Talagiu valley |
| 4 | 7734 | M13 | Aampx | whole rock | 0.830 | 3.8919*10-7 | 45.0 | 12.02±0.45 | Talagiu valley |
| 5 | 7710 | ZBA1 | Apx | whole rock | 0.839 | 4.5324*10-7 | 69.3 | 13.84±0.44 | Pleşii ridge |
| 6 | 7711 | ZBA3 | Aampx | whole rock | 0.987 | 4.1707*10-7 | 72.6 | 10.83±0.34 | Pleşii ridge |
| 7 | 7712 | ZBA4 | Aampx | whole rock | 0.968 | 3.8712*10-7 | 69.6 | 10.25±0.33 | Pleşii ridge |

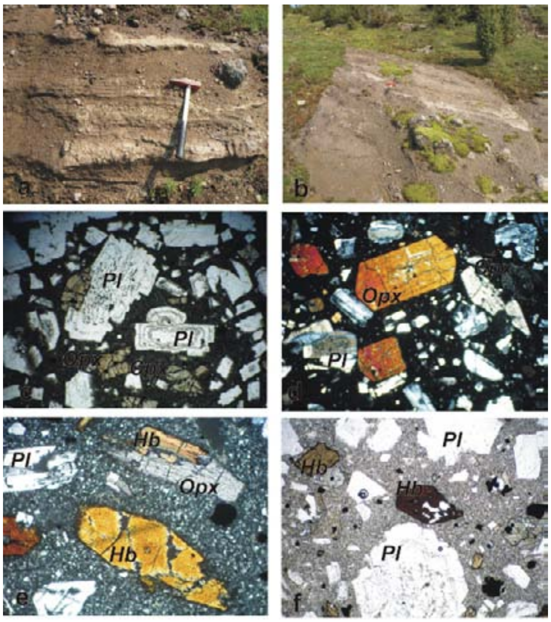

**Figure 3.** A. Diluted debris flows and fluvial deposits showing thin and cross-bedded sandstone showing of alternating coarse and fine layers with discontinuous lapilli trains, some with low angle cross laminations - south-eastern slope of the volcano; B. Well-sorted diluted debris flow fluvial deposits showing low angle cross lamination developing in lenses and pockets - south-eastern slope of the volcano; C. Micrograph of porphyritic pyroxene andesite with zoned plagioclase and pyroxene phenocrysts in a vitrophyric matrix (sample ZB1, plane-parallel light, FOV-5mm); D. Euhedral orthopyroxene (hypersthene) and plagioclase phenocrysts in a vitrophyric matrix –micrograph of sample ZB2 (cross light, FOV-5mm); E. Micrograph of porphyritic amphibole-pyroxene andesite with a fine intergranular groundmass (sample ZB3, cross light, FOV-3mm); F. Various size of the plagioclase, amphibole and pyroxene phenocrysts in a fine intergranular groundmass (micrograph of sample ZB4, plane-parallel light, FOV-5mm).

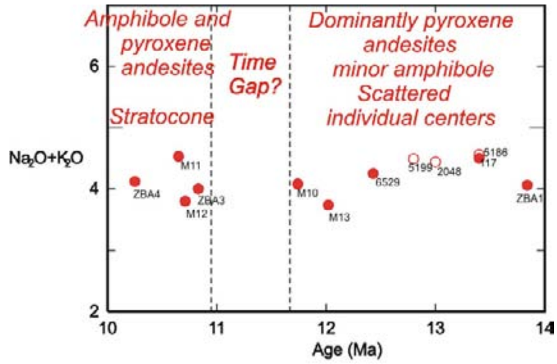


**Figure 4.** $Na_2O+K_2O$ versus K/Ar age plot of the sampled volcanic rocks belonging to the Bontău volcano and adjacent areas. Full circles represent samples from the massive rocks belonging to the volcano; open circles belong to the volcanic rocks in the neighboring areas; Source data: [1] and this work.

over hypersthene also occur. Amphibole is typical for amphibole-pyroxene andesite rocks; it is of brown-green color and rarely has reaction rims (Figure 3E). Opaque minerals are represented by magnetite, being included in all important mineral phases as well as in the groundmass (Figures 3C, F).

The geochemical considerations are based on the major oxide concentrations (Table 3). Besides our own data (analytical methods are given in the Appendix), we plotted previously published data [1] as well, belonging to this volcano, but also to adjacent volcanic structures. All the rocks plot in the andesite field in the TAS diagram, and fall in the medium-K calc-alkaline field in the $K_2O$-$SiO_2$ diagram (Figures 5A, B). Only CaO and MgO contents decrease with increasing $SiO_2$.

## 5. Discussion and conclusions

Bontău is a typical composite volcano that developed in two phases. During the first phase pyroxene andesite

**Table 3.** Major chemical analyses of the K/Ar samples.

| Sample | $SiO_2$ | $Al_2O_3$ | $Fe_2O_{3T}$ | MgO | CaO | $Na_2O$ | $K_2O$ | $TiO_2$ | MnO | $H_2O$ | Total |
|---|---|---|---|---|---|---|---|---|---|---|---|
| M10 | 60.00 | 17.40 | 6.90 | 1.80 | 7.50 | 3.25 | 0.83 | 0.96 | 0.092 | 1.24 | 99.97 |
| M11 | 59.19 | 18.20 | 6.50 | 2.80 | 6.80 | 3.40 | 1.13 | 0.64 | 0.16 | 1.44 | 100.26 |
| M12 | 57.00 | 17.41 | 7.15 | 3.43 | 8.70 | 2.94 | 0.86 | 0.91 | 0.17 | 1.37 | 99.94 |
| M13 | 56.99 | 17.10 | 8.40 | 4.80 | 7.00 | 2.78 | 0.96 | 0.73 | 0.192 | 1.07 | 100.02 |
| ZBA3 | 59.95 | 16.40 | 7.30 | 4.10 | 5.40 | 2.98 | 1.02 | 0.84 | 0.183 | 1.75 | 99.92 |
| ZBA1 | 57.56 | 15.50 | 8.40 | 6.40 | 6.50 | 2.90 | 1.16 | 0.78 | 0.182 | 0.51 | 99.89 |
| ZBA4 | 58.03 | 16.70 | 8.40 | 4.30 | 6.40 | 3.01 | 1.11 | 0.87 | 0.202 | 0.96 | 99.98 |

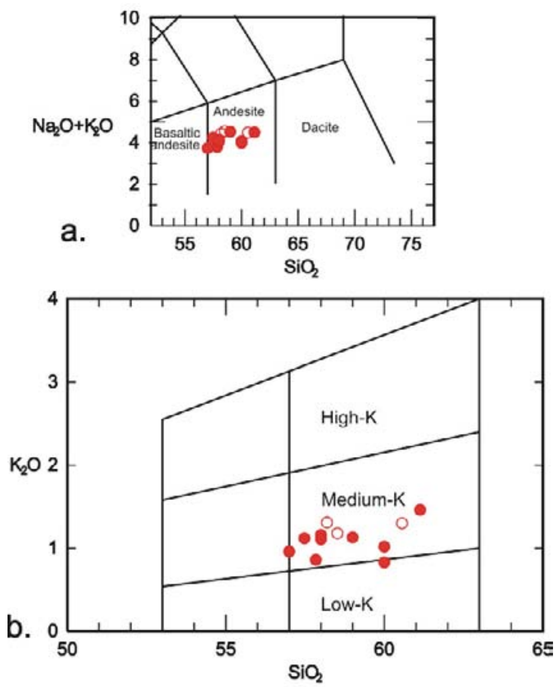


**Figure 5.** A. TAS and B. $K_2O$-$SiO_2$ diagram showing the medium-K composition of the andesites belonging to the Bontău volcano. Symbols and source data as in Figure 4.

domes generated marginal breccia (autoclastic, pyroclastic block-and-ash-flow deposits) and secondary debris flows. The eruption of the second phase was dominantly explosive and rarely non-explosive and produced volcanic domes. Large volumes of volcaniclastic deposits were produced during the second stage, suggesting an increase in both volatile content and viscosity of the magma prone to a larger production of fragmented, mainly pyroclastic material. The mixture of juvenile components such as contrasting colored pumice and scoria (attesting to variable vesicularity) in the main pyroclastic flow deposits suggest a variation in the height of the eruption column with variable intensity, depending on the increasing volatile content from strombolian to subplinian [19].

The first eruptive phase developed between 13.8-12 Ma from scattered volcanic centers, and the second one focused at the central vent area generated a cone shaped volcanic edifice between 11-10 Ma. Petrographically the second phase is built up of amphibole-pyroxene andesite. Its duration of ca. 1 Ma is rather typical for composite volcanoes elsewhere in the world [22, 23], but this was a continuation of ca. 3 Ma of prior activity roughly in the same area resulting in a number of scattered smaller volcanoes of pyroxene andesite composition. Preservation of the typical cone morphology (Figure 1) suggests that the erosion was not able to destroy its initial shape; we estimate that erosion has removed less than 1000 m during the last ~10 Myr.

The major oxide distribution along petrographical data support minor fractional crystallization processes during evolution of the magmas in crustal-level chambers, compatible with the extensional setting that not favored long stage magma chamber processes.

The volcano is similar in dimensions and length of volcanic activity with any composite volcano in subduction-related systems even though it evolved in an extensional setting. Further detailed volcanological and geochemical studies are needed to better quantify the volcano evolution.

# Acknowledgements

This paper is to be presented in the XIX Congress of the Carpathian Balkan Geological Association in Thessaloniki, 23-26 September 2010. We thank the Institute of Geodynamics, Romanian Academy for support, as well for the benefits of the academic cooperation project currently running between the Romanian Academy and the Hungarian Academy of Sciences. Z. P. and K. G. work was financially supported by the OTKA K68153 grant. I. S. is grateful to I. Berbeleac for fruitful discussions. We thank three anonymous reviewers for their excellent and constructive reviews which have significantly improved the quality of the original manuscript.

## Appendix

## Analytical methods

For major element geochemistry, 1.5-4 g of each sample was heat-sealed in teflon (FEP) foils with the sizes of about 20×30 $mm^2$. The measurements were performed at the prompt gamma activation analysis facility of the Budapest Research Reactor (BRR). The instrument is located at the end of a cold neutron beam, which is extracted from the cold neutron source of the 10 MW research reactor. The neutrons are guided 35 m away from the reactor core by means of evacuated, curved, horizontal guides without significant loss. The samples were irradiated in a cold neutron beam with a flux of 1.2×108 $cm^{-2}s^{-1}$. The cross-section of the neutron beam during the measurement was collimated to 1 $cm^2$ or to 44 $mm^2$. The neutron flux has been proved to be stable during the reactor cycles and homogeneous in the area of the beam. Because the samples are practically transparent to neutrons, average bulk compositions of the investigated volume are obtained. All the samples were thinner than 5 mm; thus the corrections for the self-absorption of neutrons and gamma-photons were negligible. The emitted gamma radiation was detected with a High Purity Germanium detector, surrounded by a Bismuth Germanate scintillator; the signals were processed with a multi-channel analyzer. The measurement system has been described by [24]. The measurement time for each individual sample varied between 1500 and 4100 s. The measurement times were set to achieve acceptable accuracies for the major components and B. The spectra were fitted with Hypermet-PC software; the element identification was performed using our prompt-gamma library [25] and evaluated with an Excel macro developed by [26].

Methodology of the whole rock K/Ar measurements used in the laboratory of the Hungarian Academy of Sciences in Debrecen: Individual rocks samples were crushed and sieved to separate the fraction 250-500 $\mu$ for Ar analysis. It was degassed by high frequency induction heating, the usual getter materials (titanium sponge, CaO, SAES getter and cold traps) being used to clean argon. A $^{39}$Ar spike was introduced to the system from a gas pipette before the degassing started. Cleaned argon was directly introduced into the mass-spectrometer. The mass spectrometer was the magnetic sector type of 150 mm radius and 90$^o$ deflection. It was operated in a static mode. Recording and evaluation of the Ar spectra was controlled by a microcomputer. To determine potassium content 0.1 g of pulverized samples were digested in HF with addition of sulfuric and perchloric acids. The digested sample was dissolved in 100 ml 0.25 mol $l^{-1}$ HCl. After a subsequent fivefold dilution 100 ppm Na and 100 ppm Li were added as a buffer and internal standard. K concentrations were measured by the digitized flame photometer OE-85 manufactured in Hungary. The interlaboratory standards Asia 1/65, LP-6, HD-B1, and GL-O as well as atmospheric Ar were used to control the measurements. Details of the instruments, applied methods, and calibration results have been published in [27].

## References

[1] Roşu E., Seghedi I., Downes H., Alderton D.H.M., Szakács A., Pécskay Z., Panaiotu C., Panaiotu C.E., Nedelcu L., Extension-related Miocene calc-alkaline magmatism in the Apuseni Mountains, Romania: origin of magmas. Swiss Bulletin of Mineralogy and Petrology, 2004, 84/1-2, 153-172

[2] Pécskay Z., Edelstein O., Seghedi I., Szakács A., Kovacs M., Crihan M., Bernad A., K-Ar datings of the Neogene-Quaternary calc-alkaline volcanic rocks in Romania. Acta Vulcanologica, 1995, 7, 53-63

[3] Roşu E., Pécskay Z., Stefan A., Popescu G., Panaiotu C., Panaiotu C.E., The evolution of the Neogene volcanism in the Apuseni Mountains (Romania): constraints from new K/Ar data. Geologica Carpathica, 1997, 48, 6, 353-359

[4] Săndulescu M., Cenozoic tectonic history of the Carpathians. In: The Pannonian Basin: A study in Basin evolution. L. Royden & F. Horvath (Eds.), AAPG Memoir, 45, 1988, 17-25

[5] Dallmeyer R.D., Pană D.I., Neibauer F., Erdmer P., Tectonothermal evolution of the Apuseni Mountains, Romania: Resolution of Variscan versus Alpine events with 40 Ar/39 Ar ages: J. Geol., 1999,107, 329–352

[6] Pană D.I., Heaman L.M., Creaser R.A., Erdmer P., Pre-Alpine Crust in the Apuseni Mountains, Romania: Insights from Sm-Nd and U-Pb Data. J. Geol., 2002, 110, 341-354

[7] Royden L.H., Late Cenozoic tectonics of the Pannonian basin system. In: The Pannonian Basin: A study in Basin evolution, L. Royden & F. Horvath (eds.), AAPG Memoir, 45, 1988, 27-48

[8] Csontos L., Márton E., Worum G., Benkovics I., Geodynamics of SW-Pannonian inselberg (Mecsek and Villany Mts., SW Hungary): inference from complex structural analysis, EGU Müller Special Pub., Ser. 3, 2002, 1-19

[9] Seghedi I., Balintoni I., Szakács A., Interplay of tectonics and Neogene post-collisional magmatism in

the Intracarpathian area. Lithos, 1998, 45, 483-499

[10] Seghedi I., Downes H., Szakács A., Mason P.R.D., Thirlwall M.F., Roşu E., Pécskay Z., Marton E., Panaiotu C., Neogene-Quaternary magmatism and geodynamics in the Carpathian-Pannonian region: a synthesis. Lithos, 2004, 72, 117-146

[11] Seghedi I., Bojar A.-V., Downes H., Roşu E., Tonarini S., Mason P.R.D., Generation of normal and adakite-like calc-alkaline magmas in a non-subductional environment: A Sr-O-H isotopic study of the Apuseni Mountains Neogene magmatic province, Romania. Chemical Geology, 2007, 245, 70-88

[12] Tari G., Dovenyi P., Dunkl I., Horvath F., Lenkey L., Ştefanescu M., Szafian P. and Toth T., Lithospheric structure of the Pannonian basin derived from seismic, gravity and geothermal data. In: Durand B., Jolivet L., Horvath F. and Serrane M. (Editors), The Mediterranean Basins: extension within the Alpine Orogen. Geol. Soc. London Spec. Publ., 156, 1999, 215-250

[13] Ianovici V., Giuşca D., Ghiţulescu T.P., Borcoş M., Lupu M., Bleahu M. and Savu H., Geological evolution of the Metaliferi Mountains Ed. Acad. Rep. Soc. România, 741 pp (in Romanian), 1969

[14] Istocescu D., Geological study of the western part of the Crişul Alb valley and Codru and Highiş border. St. Tehn. Econom. Series J, 1971, 8, pp.201 (in Romanian)

[15] Savu H. and Neacşu Gh., Neogene volcanism in the Zărand basin. D. S. Com. Geol. 1962, XLVIII, 345-360, Bucharest (in Romanian with Russian and French abstract)

[16] Berbeleac I., David M. and Zămârcă A., Petrological and petrochemical data on the Tertiary volcanics from the eastern part of the Zărand Mountains. D.S. Inst. Geol. Geofiz., 1984, LXVIII (1981), 27-46

[17] Berbeleac I., Neacşu V., Zămârcă A., Bratosin I., Geochemistry and mineralogy of altered rocks and pyrites associated with the porphyry copper-gold mineralization of the Tertiary subvolcanic from Talagiu, Zărand Mountains. Rom. J. Mineral Deposits, 1992, 75, 55-64

[18] Berbeleac I., Iliescu D., Andrei J., Ciuculescu O., Ciuculescu R., Relationships between alterations, porphyry copper-gold and base metal-gold hydrothermal vein mineralizations in Tertiary intrusions, Talagiu area, Zărand Mountains. Rom. J. Mineral Deposits, 1995, 76, 31-39

[19] Freundt A., Wilson C.J.N., Carey S.N., Ignimbrites and block-and-ash deposits. In: Sigurdsson H., Houghton B.F., McNutt S.R., Rymer H., Stix J. (Eds.), Encyclopedia of Volcanoes, Academic Press, San Diego, 2000, 581-601

[20] Davidson J., De Silva S., Composite volcanoes. In: Sigurdsson H., Houghton B.F., McNutt S.R., Rymer H., Stix J. (Eds.), Encyclopedia of Volcanoes, Academic Press, San Diego, 2000, 663-683

[21] Sagatovici A., Anastasiu N., The study of pyroclastic rocks from Minişul de sus (Bazinul Zărandului). Analele Universitaţii Bucureşti, Geologie, 1972, XXI, 31-40 (in Romanian)

[22] Morrissey M.M., Mastin L.G., Vulcanian eruptions. In: Sigurdsson, H., Houghton, B.F., McNutt, S.R., Rymer, H., Stix, J. (Eds.), Encyclopedia of Volcanoes, Academic Press, San Diego, 2000, 463-467

[23] Szakács A., Redefining active volcanoes: a discussion. Bulletin of Volcanology, 1994, 56, 321-325

[24] Belgya T., Révay Zs., Gamma-ray spectrometry. In Molnár, G.L.: Handbook of prompt gamma activation analysis with neutron beams. Kluwer Academic Publisher, 2004, 71–111

[25] Révay Zs., Belgya T., Ember P.P., Molnár G.L., Recent Developments in Hypermet-PC. J. Radioanal. Nucl. Chem., 2001, 248, 401–405

[26] Révay Zs. Determining Elemental Composition Using Prompt Gamma Activation Analysis, Anal. Chem., 2009, 81, 6851–6859

[27] Balogh K., K-Ar dating of Neogene volcanic activity in Hungary. Experimental technique, experiences and methods of chronological studies. ATOMKI Reports 1985, D/1, 277–288